

Magnetic reconnection acceleration of astrophysical jets for different jet geometries *

A-Ming Chen and Li-Ming Rui

College of Physical Science and Technology, Central China Normal University, Wuhan 430079, China; chenaming@mails.ccnu.edu.cn

Received 2014 April 10; accepted 2014 July 9

Abstract The acceleration mechanisms of relativistic jets are of great importance for understanding various astrophysical phenomena such as gamma-ray bursts, active galactic nuclei and microquasars. One of the most popular scenarios is that the jets are initially Poynting-flux dominated and succumb to magnetohydrodynamic instability leading to magnetic reconnections. We suggest that the reconnection timescale and efficiency could strongly depend on the geometry of the jet, which determines the length scale on which the orientations of the field lines change. In contrast to a usually-assumed conical jet, the acceleration of a collimated jet can be found to be more rapid and efficient (i.e. a much more highly saturated Lorentz factor can be reached) while the jets with lateral expansion show the opposite behavior. The shape of the jet could be formed due to the lateral squeezing on the jet by the stellar envelope of a collapsing massive star or the interaction of the jet with stellar winds.

Key words: gamma rays: bursts — galaxies: jets — MHD — instabilities

1 INTRODUCTION

Highly collimated, relativistic jets are widely considered to exist in many compact astronomical objects such as active galactic nuclei (AGNs), blazars and gamma-ray bursts (GRBs) (Livio 1999), whereas the physical mechanisms responsible for the acceleration and collimation of these jets are still being debated. However, observations by the *Hubble Space Telescope*, *Chandra* and VLBI, indicate that these jets are strongly related to magnetized central objects or magnetized accretion disks (Ford et al. 1994; Harms et al. 1994; Gong & Li 2012) and this mechanism is also supposed in many theoretical models (e.g., Mészáros & Rees 1997; Usov 1992; Spruit 1999; Dai et al. 2006; Yu et al. 2010; Yu & Dai 2007; Mao et al. 2010). According to these models, the magnetically-driven outflows are probably initially Poynting-flux dominated, and then the outflows must be converted to kinetic energy by some kind of acceleration mechanisms to account for the observed large bulk Lorentz factors of the order of $10^2 - 10^3$ (Fenimore et al. 1993; Woods & Loeb 1995; Lithwick & Sari 2001; Drenkhahn & Spruit 2002). A question then arises: how can the jet be accelerated to such a high speed?

As the most direct consideration, one may ascribe the jet acceleration as being due to the pressure of the associated magnetic field in the outflow. However, for a purely radial outflow, the radial

* Supported by the National Natural Science Foundation of China.

gradient of the magnetic pressure could be just balanced by the inward magnetic tension force and thus no acceleration can happen (Michel 1969). Alternatively, the rapid rotation of magnetized compact objects, due to magnetocentrifugal acceleration, acts as an ideal magnetohydrodynamic (MHD) process. This occurs when a spinning central body twists the magnetic field into a toroidal component and then the plasma is ejected by magnetic tension (Begelman & Li 1994; Daigne & Drenkhahn 2002). Unfortunately, the efficiency of such a magnetocentrifugal acceleration is always found to be too low to explain the observed high Lorentz factors (Spruit et al. 2001; Yu et al. 2009). Therefore, for the acceleration of a relativistic outflow, there must be another process that can efficiently convert the Poynting flux energy into bulk kinetic energy of the flow and accelerate the jet.

Drenkhahn (2002) has pointed out that such an efficient conversion could take place if the magnetic field in the outflow can change its direction on sufficiently small scales, because the changes in direction lead to reconnection between field lines that have opposite polarity. As a result, the Poynting-flux-dominated flow is gradually converted into a kinetic-energy-dominated one via magnetic reconnection. Simultaneously, the outflow is effectively accelerated due to the imbalance between the pressure gradient and the tension force appearing in the non-radial outflow. Furthermore, Giannios & Spruit (2006) also investigated how the bulk Lorentz factor of the jet depends on the parameters of the outflow such as energy luminosity L , baryon loading σ_0 (the initial ratio of the radial Poynting flux to kinetic energy), and different jet opening angles θ . The length scale of the alternation in the field lines also plays a crucial role in determining the acceleration rate of the flow. However, the length scale is sensitive to the configuration of the jet, which is usually simply assumed to have a conical geometry. However, previous works disregard the collimation or possible problems with lateral expansion. Nevertheless, more and more observations of relativistic jets in AGNs, radio galaxies or microquasars in the other galaxies have shown that many of these jets are not purely conical, but also exhibit other geometries, such as cylindrical (e.g., Cheng & Lu 2001; Lamb 2000; Perley et al. 1984; Biretta et al. 1999) or have trumpet-shaped jets with lateral expansion. Therefore, for a general consideration, it is necessary to investigate the acceleration of astrophysical jets for different jet geometries under the magnetic reconnection model.

In this paper we investigate the dynamics of magnetized outflows with possible evolutions of jet geometries. We describe the dynamics of jet acceleration based on the magnetic reconnection model in Section 2 and the reconnection timescales under different jet geometries are given in Section 3. The numerical results of the jet dynamics and the evolution of magnetization ratio with a brief discussion are given in Section 4.

2 ACCELERATION DUE TO MAGNETIC RECONNECTION

In this section we briefly introduce and develop a dynamical model for a magnetically-driven jet based on the model of Drenkhahn (2002). The dynamical evolution of the jet is determined by the conservations of mass and energy. The mass flux loss per time and energy flux of the outflow can be written as

$$\dot{M} = \Omega r^2 \rho u c, \quad (1)$$

$$L = \Gamma \dot{M} c^2 + \Omega \frac{(rB)^2}{4\pi} \beta c, \quad (2)$$

respectively, where $\Omega = 2\pi(1 - \cos\theta)$ is the solid angle of the jet with θ being the half opening angle, r is the radius, ρ is the mass density and u is the radial bulk 4-velocity. We use the notation Γ for the bulk Lorentz factor of the jet, and the dimensionless velocity $\beta = u/\Gamma$ for the bulk velocity in units of the speed of light c . If θ is a constant, then equations return to the case of a conical jet, which has been discussed in previous works, and disregard the possible evolution of the length scale associated with alternation of the field lines (Drenkhahn 2002; Giannios & Spruit 2006). Equation (2)

shows that the total energy of the flow consists of the bulk kinetic energy flux $L_{\text{kin}} = \Gamma \dot{M} c^2$ and the Poynting luminosity $L_{\text{pf}} = \Omega (rB)^2 \beta c / (4\pi)$. The ratio between these two components of energy is denoted by

$$\sigma = \frac{L_{\text{pf}}}{L_{\text{kin}}} = \frac{\Omega (rB)^2 \beta c}{4\pi \Gamma \dot{M} c^2} = \frac{B^2}{4\pi \Gamma^2 \rho c^2}, \quad (3)$$

which refers to the magnetization ratio of the flow (Drenkhahn & Spruit 2002; Drenkhahn 2002; Giannios & Spruit 2006). So, we can rewrite the total luminosity as $L = (1 + \sigma) \Gamma \dot{M} c^2$. The start point of our calculations will be set at the Alfvén point where the centrifugal acceleration has mostly already occurred so that the corotation of matter cannot be forced by the magnetic field. After the Alfvén point, the acceleration of the jet will be dominated by the reconnection processes. Denoting the initial magnetization degree at the Alfvén point as σ_0 , the initial 4-velocity that is defined by the Alfvén speed can be written as $u_0 = u_A(r_A) = (B/\Gamma) / \sqrt{4\pi \rho c^2} = \sqrt{\sigma_0}$ which is consistent with previous studies (Michel 1969; Goldreich & Julian 1970; Camenzind 1986; Beskin et al. 1998). Then we have $L = (1 + \sigma_0) \Gamma_0 \dot{M} c^2 = (1 + \sigma_0) \sqrt{\sigma_0} \dot{M} c^2$ for which we use the approximate expression $\Gamma_0 = \sqrt{(u_0^2 + \sqrt{u_0^4 + 4u_0^2})/2} \approx u_0$. In the ultrarelativistic case, we have $\beta \approx 1$, $u \approx \Gamma$ and $\sigma_0 + 1 \approx \sigma_0$ (Drenkhahn 2002). With these approximations, Equation (2) and Equation (3) become

$$L_{\text{pf}} = \Omega \frac{(rB)^2}{4\pi} c = L \left(1 - \frac{\Gamma \dot{M} c^2}{L} \right) \approx L \left(1 - \frac{\Gamma}{\sigma_0^{3/2}} \right), \quad (4)$$

$$\sigma = \frac{(1 + \sigma_0) \sqrt{\sigma_0}}{\Gamma} - 1 \approx \frac{\sigma_0^{3/2}}{\Gamma} - 1, \quad (5)$$

where L and σ_0 are constant model parameters. The above equation shows that the dynamic evolution of the outflow is exclusively determined by variation in the magnetic energy denoted by $(rB)^2$.

By differentiating Equation (4), the dynamical evolution of the jet can be given by

$$\frac{d\Gamma}{dr} = -\frac{1}{\Omega} \left(\sigma_0^{3/2} - \Gamma \right) \frac{d\Omega}{dr} - \frac{\Omega c}{4\pi L} \sigma_0^{3/2} \frac{d(rB)^2}{dr}, \quad (6)$$

where the first term on the right hand side is due to a possible deformation of the outflow and the latter one corresponds to an intrinsic dissipation of the field. The evolution of the magnetic field for ideal MHD is determined by the induction equation as $d(rB)/dr = 0$. By introducing a dissipation timescale τ due to magnetic reconnection, an additional dissipation term would appear in the induction equation to account for non-ideal MHD effects arising from it (Drenkhahn & Spruit 2002; Giannios & Spruit 2006)

$$\frac{d(rB)^2}{dr} = -2 \frac{(rB)^2}{c\tau} \left[1 - \mu^2 \frac{(rB)_0^2}{(rB)^2} \right], \quad (7)$$

where the parameter μ represents the initial fraction between the field strengths of the non-decaying component and the total field. Combining Equations (4), (6) and (7), we can derive the dynamical equation of the outflow as

$$\frac{d\Gamma}{dr} = \frac{2}{c\tau} \left[(\sigma_0^{3/2} - \Gamma) - \mu^2 \frac{\Omega}{\Omega_0} (\sigma_0^{3/2} - \sqrt{\sigma_0}) \right] - \frac{1}{\Omega} \frac{d\Omega}{dr} (\sigma_0^{3/2} - \Gamma). \quad (8)$$

For a conical jet with a constant value of Ω , the above equation determines a maximum Lorentz factor to be $\Gamma_{\text{max}} = \sigma_0^{3/2} (1 - \mu^2) + \sqrt{\sigma_0} \mu^2$ (more roughly, $\Gamma_{\text{max}} \sim \sigma_0^{3/2}$), which is independent of the specific magnetic dissipation mechanism denoted by the timescale τ (Drenkhahn 2002).

3 JET GEOMETRIES AND RECONNECTION TIMESCALE

The magnetic field lines with opposite directions move towards a reconnection center where the field lines are reconnected (Petschek 1964). So, the magnetic reconnection timescale should be determined by the length scale λ' on which the orientation of the field lines changes and the speed associated with the motion of field lines. Specifically, we can write

$$\tau = \Gamma \frac{\lambda'}{\varepsilon v'_A}, \quad (9)$$

where the speed of the moving field lines is considered to be proportional to the Alfvén speed v'_A by a coefficient ε (Begelman 1998; Drenkhahn 2002) and the Lorentz factor converts the timescale from the comoving rest frame to the local lab frame. Following $u'_A = \sqrt{\sigma}$ and Equation (3), the comoving Alfvén speed can be calculated by

$$v'_A = c \frac{u'_A}{\sqrt{1 + u'^2_A}} = c \sqrt{\frac{\sigma}{1 + \sigma}} \approx c \sqrt{1 - \frac{\Gamma}{\sigma_0^{3/2}}}, \quad (10)$$

which indicates that the Alfvén speed is very close to the speed of light before the magnetic reconnection is completed.

The alternation in the orientation of the field lines is probably caused by a misalignment between the axes of the magnetic moment and the rotation of the central compact object. Such a non-axisymmetric structure will lead to an azimuthal component of the magnetic field and then a helical structure could be formed, as illustrated in Figure 1. Consequently, a wave-like variation occurs at all latitudes, and the typical length scale of variation in the field is the diameter of the jet section. For the usually supposed conical jet, the alternative length scale as a function of distance r to the central object can be calculated by $\lambda' = 2r\theta$, where θ is the half opening angle of the jet. However, more generally, the opening angle of the jet is not constant. In the non-constant case, it evolves with r due to the lateral squeezing on the jet by the stellar envelope of a collapsing massive stars or the interaction of the jet with stellar winds. Following such a consideration, a power-law evolution of the opening angle as $\theta = \theta_0 (r/r_0)^\alpha$ is assumed to be the lowest order of approximation. Then the length scale can be written as

$$\lambda' = 2r\theta_0 \left(\frac{r}{r_0} \right)^\alpha. \quad (11)$$

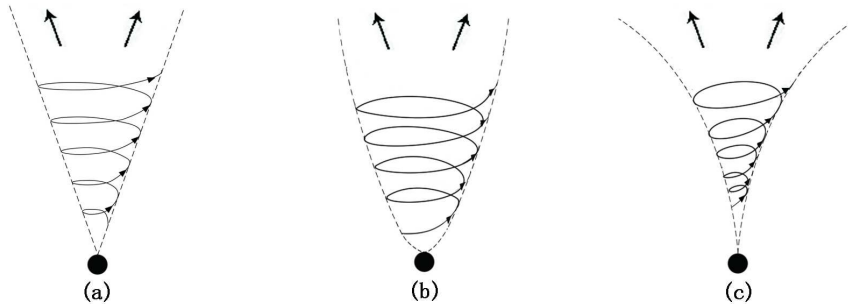


Fig. 1 Illustrations of different structures (conical, parabolic and trumpet-like shapes) for the magnetic field of the jet.

Different values for the index α determine different jet geometries, e.g. a collimated jet for $-1 < \alpha < 0$, a trumpeted jet for $0 < \alpha < 1$ and the usual conical jet for $\alpha = 0$. A cylindrical jet with a constant cross section can be described as a limiting case of $\alpha = -1$. Illustrations of the different jet geometries are presented in Figure 1.

4 RESULTS AND DISCUSSION

Generally speaking, the model presented above is viable in both situations of AGNs and GRBs, although the length scales of the two types of objects are completely different. Specifically, the central black holes harbored in AGNs are supermassive, on the order of $10^6 - 10^{10} M_\odot$, whereas objects at the centers of GRBs are stellar-mass black holes or magnetars. Therefore, the initial and typical radius of the AGN jets must be much larger than the GRB jets. On the other hand, the Lorentz factors of the AGN jets could be somewhat lower than the GRB ones. However, the conversion of magnetic energy to kinetic energy of the jets, which is the focus of this paper, could be qualitatively similar between the AGNs and GRBs. In the following calculations, we take parameter values typical for GRB jets just as an example, i.e. the initial magnetization of the jet with $\sigma_0 = 100$ at the Alfvén point $r_0 \sim 10^7$ cm, $\epsilon = 0.1$ and $\mu^2 = 0.5$. More specifically, such parameters are potentially related to a GRB with a central magnetar.

The numerical results of the dynamic and magnetization evolution of jets with a parabolic jet structure (a collimated jet) and a trumpet-like jet structure (with lateral expansion) for the magnetic field profile are given in Figures 2 – 5. As a comparison, the case of a usual conical jet (with a half opening angle $\theta = 5^\circ$) is also shown by the solid line, which can be approximatively described by the following analytic solution given by Drenkhahn (2002)

$$\Gamma \approx \left[\frac{2\epsilon(1-\mu^2)\sigma^{3/2}}{\theta} \ln\left(\frac{r}{r_0}\right) + \sigma_0 \right]^{1/2}. \quad (12)$$

As a general impression, one can see that the magnetic reconnection acts efficiently and accelerates the jet 2–3 orders of magnitude near the Alfvén point. In Figure 2, the acceleration of the parabolic jets ($\alpha < 0$) could be much more rapid and efficient (a much higher Lorentz factor can be reached) than the conical jet, whereas the trumpet-like jets ($\alpha > 0$) can only be accelerated at the very early phase and finally reach a Lorentz factor with a relatively low saturation. The jet accelerations are also strongly dependent on the initial opening angle θ_0 as shown in Figure 4. For smaller initial opening angles, the jet is accelerated faster and to a higher terminal Lorentz factor. Such a result can be understood in that a narrower jet would exhibit a much shorter reconnection timescale and thus much faster magnetic dissipation.

Another important quantity is the Poynting to matter energy flux ratio σ as a function of distance r as is shown in Figures 3 and 5. While the flow is initially moderately Poynting flux dominated, the σ drops rapidly with distance r and the flow is matter-dominated at distances $r_\infty \sim 10^{16}$ cm where the GRB jet is expected to run into the external medium. In Figures 3 and 5, we can find that collimated jets with smaller opening angles lead to lower values of σ_∞ , which means practically all the magnetic energy has been transferred to the matter.

This work suggests that the jet geometries also play a significant role in the dynamics of the outflow. The energy dissipated by magnetic reconnection accelerates the flows so that it becomes dominated by kinetic flux dominated at large distance. Our results indicate that, for acceleration of a jet that results from efficient magnetic reconnection, the profile of the jet is inclined to be parabolic. Such a configuration could be formed due to the lateral squeezing on the magnetic field by the pressure of materials encircling the jet. For example, for long GRBs originating from the collapse of massive stars, the jet driven by the central engine should firstly penetrate the stellar envelope. In such a case, the large gas pressure of the envelope laterally acting on the jet can significantly squeeze the jet, and thus enhance acceleration of the jet. For completeness of the model, we also consider a jet

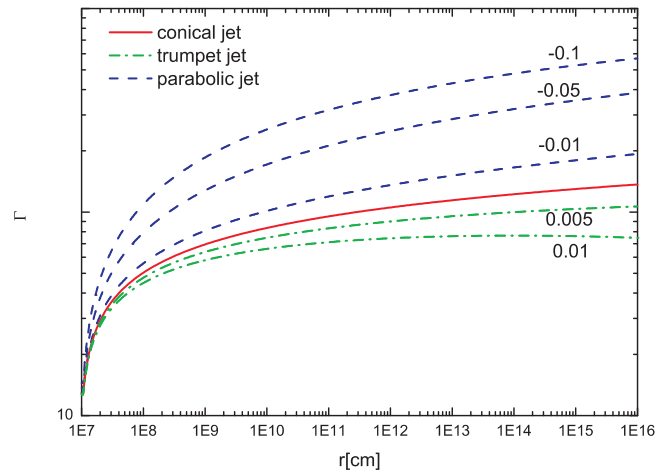


Fig. 2 The bulk Lorentz factor Γ of the jet as a function of the distance r to the central object for different values of α as labeled while keeping the initial half opening angle $\theta_0 = 5^\circ$. The dashed and dash-dotted lines correspond to parabolic and trumpet-like shapes of the jet respectively. The red solid lines correspond to the conical jet with half opening angle $\theta = 5^\circ$.

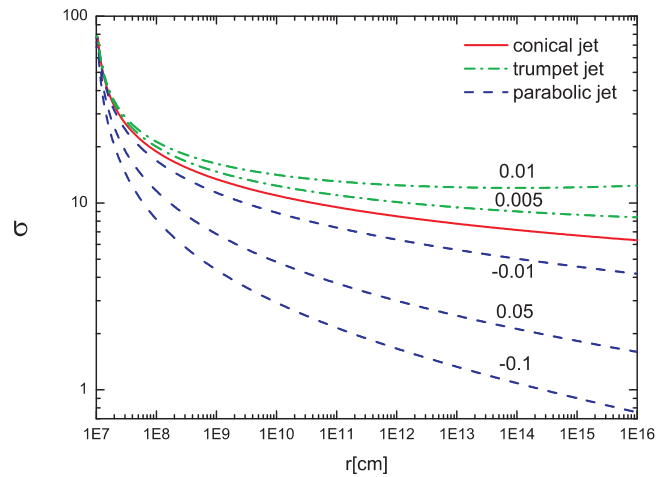


Fig. 3 The dependence of the magnetization ratio σ on distance r for different values of α while fixing $\theta_0 = 5^\circ$. The dashed and dash-dotted lines correspond to parabolic and trumpet-like shapes of the jet respectively. The red solid lines correspond to the conical jet with half opening angle $\theta = 5^\circ$.

with a trumpet-like structure that has lateral expansion, which may possibly be caused by interaction of the jet with stellar winds or other complicated boundary environments.

For a simple approach, the thermal energy is ignored in our calculations, which could slightly slow the acceleration of the jet (Begelman 1998). This approximation is quite good in the optically thick region since no energy can be radiated away (Drenkhahn 2002). However, if one wants to further consider the radiation of the jet in the optically thin region, such internal energy must to be taken into account.

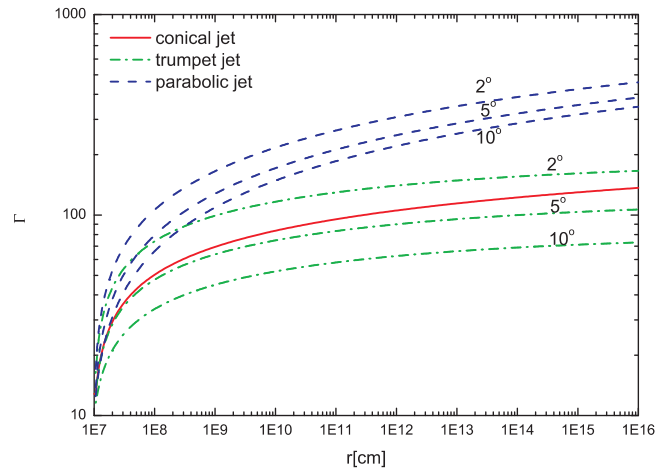


Fig. 4 The bulk Lorentz factor Γ of the jet as a function of the distance r to the central object for different values of θ_0 as labeled while fixing $\alpha = -0.05$ for the parabolic jet and $\alpha = 0.005$ for the trumpet-like jet. The dashed and dash-dotted lines correspond to parabolic and trumpet-like shapes of the jet respectively. The red solid lines correspond to the conical jet with half opening angle $\theta = 5^\circ$.

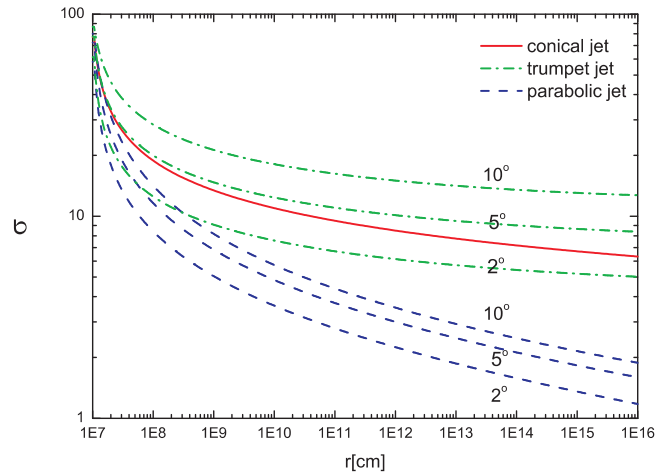


Fig. 5 The dependence of the magnetization ratio σ on distance r for different values of θ_0 while fixing $\alpha = -0.05$ for parabolic jets and $\alpha = 0.005$ for trumpet-shaped jet. The dashed and dash-dotted lines correspond to parabolic and trumpet-like shapes of the jet respectively. The red solid lines correspond to the conical jet with half opening angle $\theta = 5^\circ$.

Acknowledgements The authors thank the instruction of Yun-Wei Yu who motivated this work. This work is supported by the National Natural Science Foundation of China (Grant No. 11103004), the Foundation for the Authors of National Excellent Doctoral Dissertations of China (Grant No. 201225) and the Program for New Century Excellent Talents in University (Grant No. NCET-13-0822).

References

- Begelman, M. C., & Li, Z.-Y. 1994, *ApJ*, 426, 269
- Begelman, M. C. 1998, *ApJ*, 493, 291
- Beskin, V. S., Kuznetsova, I. V., & Rafikov, R. R. 1998, *MNRAS*, 299, 341
- Biretta, J. A., Sparks, W. B., & Macchetto, F. 1999, *ApJ*, 520, 621
- Camenzind, M. 1986, *A&A*, 162, 32
- Cheng, K. S., & Lu, Y. 2001, *MNRAS*, 320, 235
- Dai, Z. G., Wang, X. Y., Wu, X. F., & Zhang, B. 2006, *Science*, 311, 1127
- Daigne, F., & Drenkhahn, G. 2002, *A&A*, 381, 1066
- Drenkhahn, G. 2002, *A&A*, 387, 714
- Drenkhahn, G., & Spruit, H. C. 2002, *A&A*, 391, 1141
- Fenimore, E. E., Epstein, R. I., & Ho, C. 1993, *A&AS*, 97, 59
- Ford, H. C., Harms, R. J., Tsvetanov, Z. I., et al. 1994, *ApJ*, 435, L27
- Giannios, D., & Spruit, H. C. 2006, *A&A*, 450, 887
- Goldreich, P., & Julian, W. H. 1970, *ApJ*, 160, 971
- Gong, X., & Li, L. 2012, *Science China Physics, Mechanics, and Astronomy*, 55, 880
- Harms, R. J., Ford, H. C., Tsvetanov, Z. I., et al. 1994, *ApJ*, 435, L35
- Lamb, D. Q. 2000, *Phys. Rep.*, 333, 505
- Lithwick, Y., & Sari, R. 2001, *ApJ*, 555, 540
- Livio, M. 1999, *Phys. Rep.*, 311, 225
- Mao, Z., Yu, Y. W., Dai, Z. G., Pi, C. M., & Zheng, X. P. 2010, *A&A*, 518, A27
- Mészáros, P., & Rees, M. J. 1997, *ApJ*, 482, L29
- Michel, F. C. 1969, *ApJ*, 158, 727
- Perley, R. A., Bridle, A. H., & Willis, A. G. 1984, *ApJS*, 54, 291
- Petschek, H. E. 1964, *Magnetic Field Annihilation*, Tech. rep., in: WN Hess (Ed.), *AAS-NASA Symposium on the Physics of Solar Flares*, NASA SP-50, NASA, Washington, DC (1964), 425
- Spruit, H. C. 1999, *A&A*, 341, L1
- Spruit, H. C., Daigne, F., & Drenkhahn, G. 2001, *A&A*, 369, 694
- Usov, V. V. 1992, *Nature*, 357, 472
- Woods, E., & Loeb, A. 1995, *ApJ*, 453, 583
- Yu, Y. W., & Dai, Z. G. 2007, *A&A*, 470, 119
- Yu, Y. W., Wang, X. Y., & Dai, Z. G. 2009, *ApJ*, 692, 1662
- Yu, Y.-W., Cheng, K. S., & Cao, X.-F. 2010, *ApJ*, 715, 477